Biochemistry

 Volume 33, Number 14 April 12, 1994

Accelerated Publications

^{15}N NMR Relaxation Studies of the FK506 Binding Protein: Dynamic Effects of Ligand Binding and Implications for Calcineurin Recognition

Jya-Wei Cheng,‡ Christopher A. Lepre, and Jonathan M. Moore*

Vertex Pharmaceuticals Incorporated, 40 Allston Street, Cambridge, Massachusetts 02139-4211

Received December 27, 1993; Revised Manuscript Received February 7, 1994®

ABSTRACT: Backbone dynamics of the ligand- (FK506-) bound protein FKBP-12 (107 amino acids) have been examined using ^{15}N relaxation data derived from inverse-detected two-dimensional ^{1}H–^{15}N NMR spectra. A model free formalism [Lipari & Szabo (1982) *J. Am. Chem. Soc. 104*, 4546–4559] was used to derive the generalized order parameter (S^2), the effective correlation time for internal motions (τ_e), and the chemical-exchange line width (R_{ex}) based on the measured ^{15}N relaxation rate constants (R_1, R_2) and ^{1}H–^{15}N heteronuclear NOEs. The final optimized overall correlation time (τ_m) was 9.0 ns. The average order parameter (S^2) describing the amplitude of motions on the picosecond time scale was found to be 0.88 ± 0.04, indicating that internal flexibility is restricted along the entire polypeptide chain. In contrast to results obtained for uncomplexed FKBP, the 80's loop (residues 82–87) surrounding the ligand binding site was found to be rigidly fixed, indicating that internal motions at this site are damped significantly due to stabilizing noncovalent interactions with the FK506 molecule. Structural implications of these differences in picosecond mobility as well as possible implications for calcineurin recognition are discussed.

FKBP-12[1] (M_r = 11 800) belongs to a family of immunomodulatory proteins termed immunophilins (Schreiber, 1991; Rosen & Schreiber, 1992; Sigal & Dumont, 1992). The most widely characterized immunophilins include FKBP-12 and cyclophilin (M_r = 17 000). These two proteins, which share no amino acid sequence or structural similarities, both catalyze the interconversion of the *cis–trans* rotamers of peptidyl–prolyl amide bonds and are the major intracellular receptors for the potent immunosuppressants FK506 and cyclosporin A (CsA), which bind to FKBP-12 and cyclophilin (CyP), respectively. Both immunosuppressants appear to act by blocking signal transduction pathways leading to T-cell activation.

Following their discovery as receptor proteins for FK506 and cyclosporin A, FKBP-12 and cyclophilin became attractive targets for inhibitor design via a structure-based approach (Baldwin et al., 1989; Appelt et al., 1991; Kuntz, 1992; Navia & Murcko, 1992). As a result, initial synthetic strategies focused on the design of tight-binding compounds whose putative effects would be exerted through inhibition of isomerase activity. However, the results of several subsequent investigations turned what was believed to be a straightforward exercise in structure-based inhibitor design into a significantly more challenging problem.

Bierer et al. (1990), using a truncated analog of FK506 with high binding affinity for FKBP-12, demonstrated that inhibition of the peptidyl–prolyl *cis–trans* isomerase activity of FKBP-12 was not sufficient for immunosuppression, implying that it was not the isomerase activity of the uncomplexed immunophilin but rather another unknown

* Author to whom correspondence should be addressed.
‡ Present address: Department of Chemistry, BG-10, University of Washington, Seattle, WA 98195.

® Abstract published in *Advance ACS Abstracts*, March 15, 1994.

[1] Abbreviations: CPMG, Carr–Purcell–Meiboom–Gill; CSA, chemical shift anisotropy; CsA, cyclosporin A; CN, calcineurin; Cyp, cyclophilin ($M_r \sim 17\,700$); FKBP-12, FK506 binding protein ($M_r \sim 11\,800$); GARP, globally optimized alternating-phase rectangular pulses; NMR, nuclear magnetic resonance; NOE, nuclear Overhauser enhancement; R_1, longitudinal relaxation rate constant; R_2, transverse relaxation rate constant; T_1, longitudinal relaxation time; T_2, transverse relaxation time; TPPI, time proportional phase incrementation.

0006-2960/94/0433-4093$04.50/0

property of the immunophilin/drug complex which was responsible for eliciting the observed immunosuppressive effect. Subsequently, it was discovered that both the FK506/FKBP-12 and CsA/CyP complexes bind to and inhibit a common downstream target, the Ca^{2+}- and calmodulin-dependent protein phosphatase calcineurin (CN) (Liu et al., 1991). These findings profoundly influenced structure-based strategies for inhibitor design. In order to achieve immunosuppression through an FKBP-12-mediated pathway, it became necessary to design an inhibitor which binds tightly to two target proteins simultaneously. Not only must one create a small molecule to bind tightly to FKBP-12, but also one must engineer an FKBP-12/inhibitor surface which has a high affinity for the inhibitory site(s) of calcineurin.

Although the FKBP-12/FK506 complex has been well characterized by X-ray crystallographic (Van Duyne et al., 1991, 1993) and NMR methods (Lepre et al., 1992, 1993), there exists at present no three-dimensional structural information for the FK506/FKBP-12/CN ternary complex. However, studies employing chemical modification of FK506 (Liu et al., 1992) and site-directed mutagenesis of FKBP-12 (Aldape et al., 1992; Rosen et al., 1993; Yang et al., 1993) have revealed that the solvent-exposed regions of FK506 as well as nearby FKBP-12 residues are important in CN inhibition. Since it is the composite surface of the FKBP-12/FK506 complex that is interacting with CN and is responsible for eliciting an immunosuppressive response, a prerequisite in attempting the design of new inhibitors is to rigorously characterize both structurally and dynamically the interface that is presented by the protein/drug complex to calcineurin.

Since biochemical events such as substrate or inhibitor binding may induce structural and motional changes within proteins, any model used in a structure-based approach for inhibitor design should incorporate high-resolution structural information as well as dynamic aspects of a potential drug target. High-resolution structural data may be obtained through the familiar techniques of X-ray crystallography and multidimensional solution NMR spectroscopy. However, only recently, due to the development of proton-detected heteronuclear NMR relaxation methods, has it been possible to rigorously characterize the fast (picosecond) backbone dynamics of proteins, and a number of reports have appeared which examine both the internal and overall motions of small proteins [reviewed in Palmer (1993) and Wagner (1993)].

NMR methods for assessing protein dynamics are a powerful new tool in the characterization of potential drug targets via a structure-based approach. The static, yet high-resolution structural data obtained from X-ray crystallographic and NMR measurements may be augmented by experimentally derived dynamic information to provide a more realistic picture of a protein target under conditions which more accurately reflect the true biological milieu. In previous studies, we have used ^{15}N relaxation methods to characterize the backbone dynamics of uncomplexed FKBP-12 on the picosecond time scale (Cheng et al., 1993), as well as ^{13}C relaxation methods to examine the mobility of methine sites in bound FK506 (Lepre et al., 1993). To better understand the changes in protein dynamics that occur when FK506 binds to FKBP-12, and to construct a more complete dynamic model of the FKBP-12/FK506 system, we have used inverse-detected two-dimensional ^{1}H–^{15}N NMR experiments to examine the backbone dynamics of FKBP-12 in complex with FK506. Amide ^{15}N relaxation data were analyzed using the model free formalism of Lipari and Szabo (1982a,b) and interpreted in terms of the generalized order parameter (S^2), the effective correlation time for fast internal motions (τ_e), and the chemical-exchange line width (R_{ex}). Dynamic effects of ligand binding upon the protein backbone, as well as possible implications of protein and ligand dynamics upon calcineurin recognition, will be discussed.

MATERIALS AND METHODS

Sample Preparation. Uniformly ^{15}N and ^{13}C isotopically labeled human recombinant FKBP-12 was produced in *Escherichia coli* and purified as described previously (Cheng et al., 1993). The final NMR sample contained 7.9 mM human recombinant FKBP-12 in 50 mM potassium phosphate buffer (90% H_2O, 10% D_2O) at pH 7.0. ^{15}N incorporation was >95% and ^{13}C incorporation was 60–70% as determined by examination of resolved resonances in decoupled (^{15}N and ^{13}C) and nondecoupled 1D NMR spectra.

NMR Spectroscopy. All NMR experiments were recorded at 500.13 MHz (^{1}H) and 50.68 MHz (^{15}N) on a Bruker AMX-500 spectrometer equipped with a three-channel interface and triple-resonance probe. All measurements were carried out at 303 K. Pulse sequences, parameters for data acquisition, and parameters for data processing were identical to those used previously (Cheng et al., 1993). For the T_1 experiments, eight delays of 43, 195, 346, 562, 973, 1513, 2054, and 2594 ms were used during the inversion–recovery period, whereas eight delays of 19, 35, 57, 95, 133, 171, 228, and 304 ms were used during the CPMG period of the T_2 experiments.

Determination of ^{15}N Relaxation Parameters. The relaxation rate constants (R_1, R_2) were determined from nonlinear least squares fits of the experimental peak heights as described previously (Cheng et al., 1993). Uncertainties in peak heights were determined from the RMS baseline noise level and ranged from 1.5% to 3.5% of the total peak height. Heteronuclear NOEs were calculated and errors estimated as described previously (Cheng et al., 1993).

Model Free Calculations. The spin relaxation of a peptide amide ^{15}N nucleus is dominated by the dipolar interaction between the ^{15}N nucleus and the attached ^{1}H nucleus, as well as the chemical shift anisotropy (CSA). As described previously (Cheng et al., 1993), contributions to ^{15}N relaxation via carbon–nitrogen mechanisms in the partially ^{13}C-labeled sample are negligible. The ^{15}N longitudinal (R_1) and transverse (R_2) relaxation rate constants and the heteronuclear NOEs are dependent on the values of the spectral density function at five characteristic frequencies. As the number of experimental observables (R_1, R_2, NOE) are insufficient to explicitly determine the five spectral density values, a simpler model for the spectral density may be invoked. As described in detail elsewhere (Lipari & Szabo, 1982a,b; Clore et al., 1990), the model free approach characterizes both the rate and amplitude of internal motion for individual N–H bond vectors using two parameters. The effective correlation time (τ_e) depends on the rate of motion for fluctuations of the amide bond vector occurring on time scales faster than the overall rotational correlation time (τ_m) of the molecule. The generalized order parameter (S^2) is a dimensionless parameter describing the spatial extent of motion of the N–H bond unit vector. Values for the generalized order parameter may range from $S^2 = 0$, indicating completely isotropic motion, to $S^2 = 1$, describing completely restricted motion. An additional parameter, R_{ex}, may also be invoked to represent contributions to the ^{15}N transverse relaxation rate due to chemical exchange and/or conformational averaging on a time scale much slower than the overall rotational correlation time.

The model free formalism may be applied to describe the motions of either isotropically or anisotropically reorienting proteins in solution. Since the three principal components of the inertial tensor of the FKBP-12/FK506 complex were calculated to be approximately 1.0:0.90:0.97 from the X-ray crystallographic structure (Van Duyne et al., 1991), we may treat this complex as an isotropically tumbling species.

From the model free formalism, the spectral density function for an isotropically tumbling protein is

$$J(\omega) = \left(\frac{2}{5}\right)\left[\frac{S^2\tau_m}{1 + (\omega\tau_m)^2} + \frac{(1 - S^2)\tau}{1 + (\omega\tau)^2}\right] \quad (1)$$

where

$$1/\tau = 1/\tau_m + 1/\tau_e$$

If the time scale of the internal motions is fast ($\tau_e < 10$ ps), then the spectral density function of eq 1 can be reduced to

$$J(\omega) = \left(\frac{2}{5}\right)\left[\frac{S^2\tau_m}{1 + (\omega\tau_m)^2}\right] \quad (2)$$

The model free parameters were obtained by substitution of either eq 1 or eq 2 into equations describing the dependence of the relaxation rate constants R_1 and R_2 and the heteronuclear NOE on the spectral density values, followed by optimization using the experimental measurements of R_1, R_2, and the heteronuclear NOE as described previously (Cheng et al., 1993). Reliability of the fits was judged by comparing the R_1, R_2, and NOE values obtained from Monte Carlo simulations with the experimental data. Optimizations were carried out using software provided by Dr. Arthur G. Palmer, III, Columbia University, following previously published procedures (Cheng et al., 1993).

RESULTS

The ^{15}N and ^1H chemical shift assignments for the amide resonances of the FK506/FKBP-12 complex were obtained by using routine sequential assignment methods based upon two- and three-dimensional ^1H–^1H and ^1H–^{15}N NMR experiments (C. A. Lepre, J.-W. Cheng, and J. M. Moore, unpublished results). The amide assignments for FK506/FKBP-12 under present experimental conditions are nearly identical to those reported recently for the ascomycin/FKBP-12 complex (Xu et al., 1993). Of the 99 backbone amide protons (107 minus 7 Pro and N-terminal Gly), all but A84 and G89 can be found in the {^1H}–^{15}N heteronuclear NOE experiments. Among them, 11 are unresolved due to overlap. In addition, V2, D41, and V55 exhibited weak intensities in the T_1 and T_2 experiments, most likely due to amide proton exchange with solvent during the presaturation period, and were excluded from further analysis. Therefore, quantitative analysis could be made for 83 backbone amide groups.

Determination of ^{15}N Relaxation Parameters. Relaxation rate constants R_1 and R_2 were obtained from monoexponential decay fits of cross-peak height versus relaxation delay in the T_1 and T_2 experiments. The standard deviations of the fitted R_1 and R_2 values were all less than 10%, with the majority being less than 5%. The mean spin–lattice relaxation rate constant, R_1, was 1.70 ± 0.13 s^{-1}. Only six residues, F15, K44, G62, M66, K105, and E107, were found to have R_1 values smaller than the mean by one standard deviation or more. The mean value for the transverse relaxation rate constant, R_2, was 11.76 ± 0.87 s^{-1}. Values ranged from 9.79 s^{-1} for L104 to 13.89 s^{-1} for Y63. For most of the residues, including the N and C termini, NOE values were observed to be larger than 0.75, indicating that internal motions on the fast (picosecond) time scale are restricted. Experimental values for ^{15}N longitudinal (R_1) and transverse (R_2) relaxation rates and the {^1H}–^{15}N NOE are plotted as a function of residue number in Figure 1.

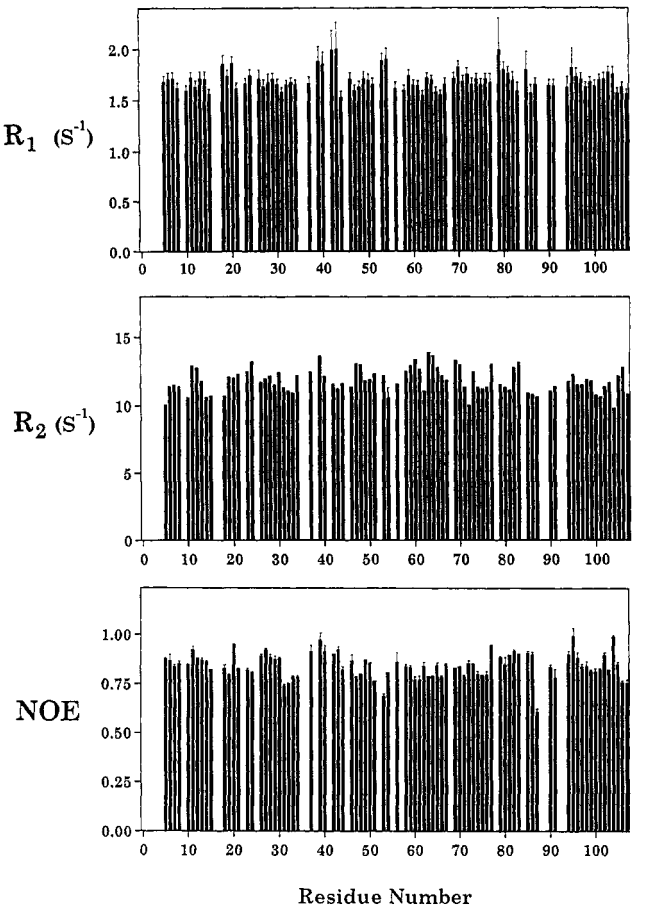

FIGURE 1: Plots of the measured ^{15}N relaxation parameters as a function of residue number: (top) spin–lattice relaxation rate constant (R_1); (middle) spin–spin relaxation rate constant (R_2); (bottom) heteronuclear NOE. Error bars represent standard deviations calculated from the covariance matrix of the optimized two- or three-parameter fit and validated by comparison to the Monte Carlo simulations (Palmer et al., 1991). Residues for which no results are shown correspond either to proline residues or to residues for which N–H cross-peaks were overlapped or could not be observed.

Initial Estimation of the Overall Rotational Correlation Time. Initial determination of the overall rotational correlation time, τ_m, was carried out as described previously (Cheng et al., 1993) on the basis of the average R_2/R_1 ratio (Kay et al., 1989) and was found to be 9.3 ns. This value compares well with the value of 9.2 ns obtained for uncomplexed FKBP-12, using a sample of similar concentration (8.6 mM) (Cheng et al., 1993), and is consistent with the fact that no large-scale structural changes occur due to ligand binding.[2]

Analysis of Model Free Parameters. Optimizations to determine the model free parameters were carried out as described previously (Cheng et al., 1993). Differences between simulated and experimental results were typically less than

[2] The values of τ_m for uncomplexed and complexed FKBP-12 are significantly longer than the value for τ_m (6.2 ns) obtained in a recent ^{13}C dynamics study of FK506 bound to FKBP-12 at a concentration of 2.8 mM (Lepre et al., 1993). These results together suggest that this longer value for τ_m most likely arises due to solution viscosity effects in such a concentrated (7.9 mM) NMR sample.

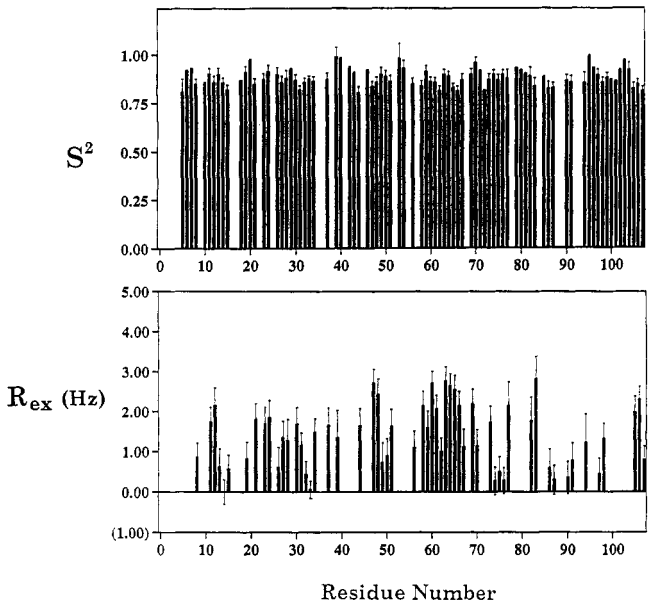

FIGURE 2: Plots of the optimized model free parameters as a function of residue number: (top) generalized order parameter (S^2); (bottom) chemical-exchange line width (R_{ex}) in hertz. Standard deviations are estimated from the Monte Carlo simulations (Palmer et al., 1991).

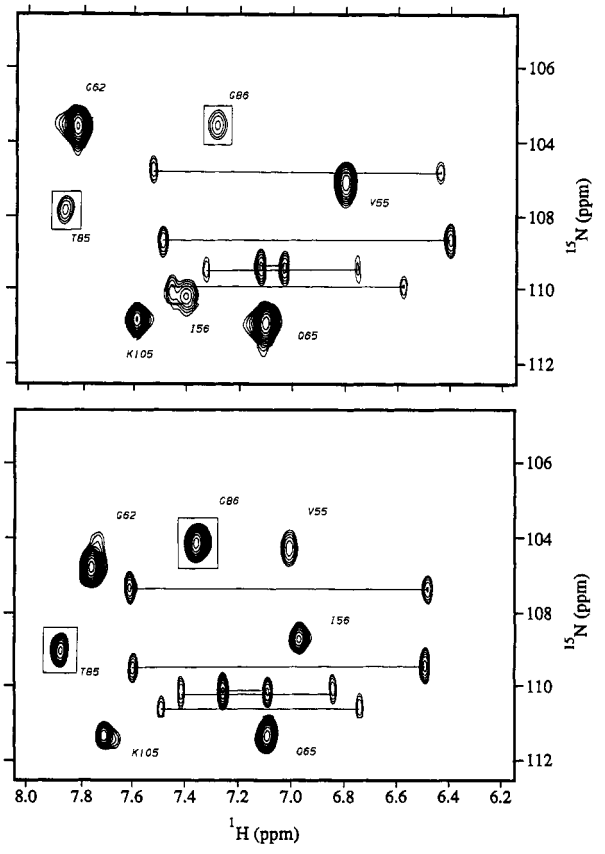

FIGURE 3: Contour plots of a region containing T85 and G86 of the first T_1 experiment for uncomplexed FKBP-12 (top) and FK506-bound FKBP-12 (bottom). Pairs of side-chain amine protons are joined by lines. T85 and G86 are boxed in each spectrum.

10%. Residual values (Γ_i^2) were less than 1.0 for 73 of 83 residues included in the final optimization, with no residual value greater than 8.77. Final optimized S^2 and R_{ex} values are shown in Figure 2 as a function of residue number. The average value of the generalized order parameter for the FK506-bound FKBP-12 is 0.88 ± 0.04. With the exception of proline residues or other residues for which resonance overlap or low peak intensity precluded detailed analysis, no order parameter less than 0.80 was found, indicating that picosecond time-scale motions are restricted throughout the entire protein backbone. For residues where an R_{ex} term was included in the optimization, all R_{ex} values were less than 3 Hz, suggesting that motions on the millisecond to microsecond time scale which result in ^{15}N T_2 line broadening, such as those arising from chemical exchange or conformational averaging, are limited.

As discussed by Palmer et al. (1991), calculation of τ_e may be unreliable in some instances. In their work, these authors found that precision in the values determined for τ_e was dependent on S^2 values, with the lower uncertainties occurring for low S^2 values and the highest (on the order of 100%) arising for S^2 values greater than 0.8. We observe similar results in this study, as several residues for which τ_e was optimized in the final calculation exhibit mean values in the simulated data which appear strongly biased compared to the optimized values. In this study we do not consider τ_e to be meaningful for residues in which the optimized values appear biased, or if the 95% confidence intervals for the simulated R_1, R_2, and NOE values do not bracket the experimental values. Using the above criteria, nonzero values for τ_e are observed for 24 N–H bond vectors. All values are under 30 ps, with the exception of Ala 72 (36 ± 30 ps) and His 87 (79 ± 18 ps). Due to the uncertainties outlined above for determination of τ_e, we have chosen not to attempt a quantitative interpretation of τ_e values.

DISCUSSION

Comparison of the Backbone Dynamics of Uncomplexed and FK506-Bound FKBP-12. We have previously examined the backbone dynamics of uncomplexed FKBP-12 (Cheng et al., 1993). The average order parameter observed for this protein was 0.88 ± 0.06, reflecting low mobility of nearly all backbone amides, except for several in the 80's loop (residues 82–87). For residues 83 and 86–87, the order parameters were lower (average S^2 = 0.74), indicating that the 80's loop of the uncomplexed protein is significantly more mobile on the picosecond time scale. In addition, the amide resonances of residues 82, 84, 85, and 86 were weak in intensity or absent (Figure 3), which can be attributed to high solvent exposure and mobility within this loop region.

Like native FKBP-12, the FK506/FKBP-12 complex has an overall rotational correlation time of 9 ns and an average order parameter for backbone amides of 0.88 ± 0.04. This result indicates that, for the most part, internal motions on the picosecond time scale are restricted in both states and that FK506 binding does not induce any conformational changes large enough to change the overall tumbling behavior of the protein. In contrast, however, the amide order parameters in the 80's loop of FK506-bound FKBP-12 (average S^2 = 0.86) are significantly higher than those measured in the uncomplexed protein, and most of the amide resonances exhibit normal intensities (Figure 3). These changes, as illustrated graphically in Figure 4, indicate clearly that picosecond time-scale motions of the 80's loop decrease significantly in amplitude when FK506 is bound. Since the model free approach describes the amplitude of the motions, but not their physical nature, it is often useful to interpret the observed generalized order parameters within the framework of a particular motional model. For example, using the diffusion-in-a-cone model (Lipari & Szabo, 1980, 1981), the increases in order parameter observed for residues Gly 86 and His 87 correspond to decreases in the cone semiangle from 30° to

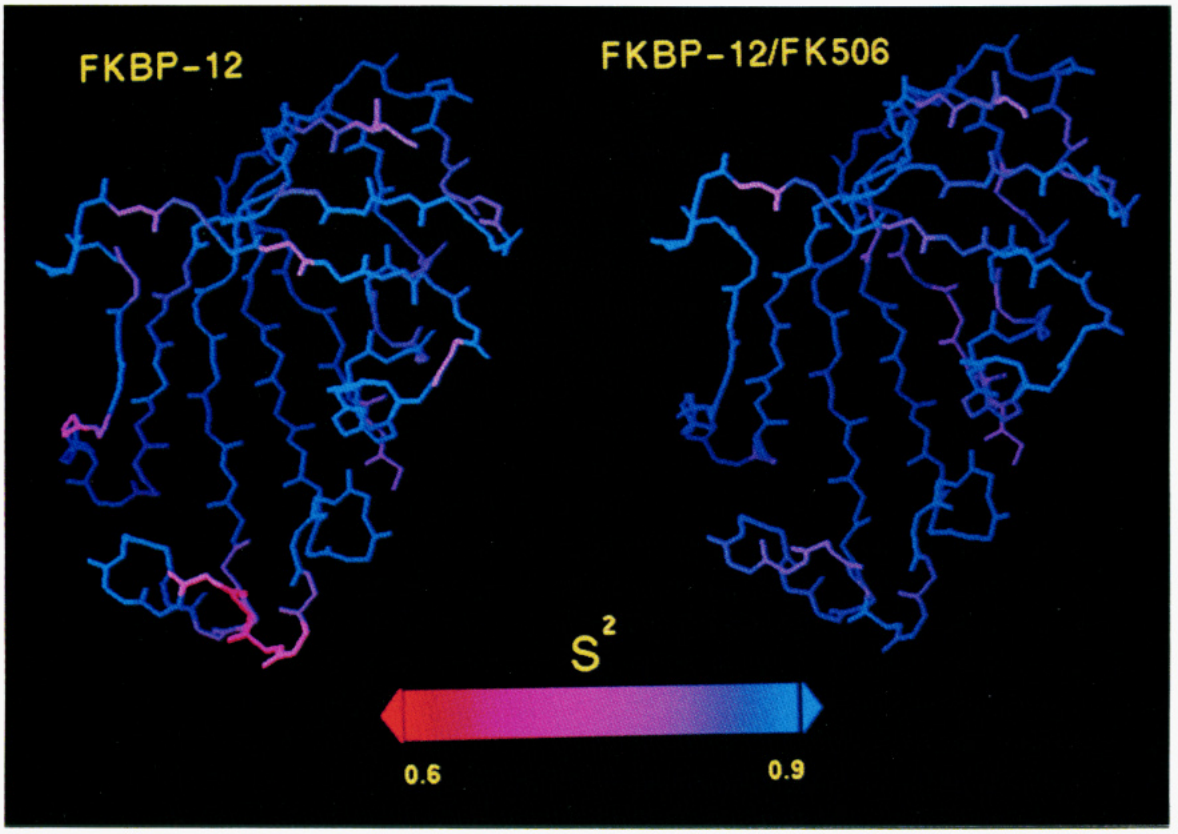

FIGURE 4: Backbone structures of uncomplexed FKBP-12 (left) and FK506-bound FKBP-12 (right) colored according to the optimized order parameter S^2. The spectrum bar below the structures indicates the color range and the values encompassed by each spectrum. Residues for which S^2 was not determined are colored according to an interpolated value based on the preceding and following residues.

19° and 24° to 19°, respectively. The reduced amplitudes of motion for amide bond vectors in the 80's loop are likely due to the formation of stabilizing contacts between the loop residue side chains and tightly bound (K_i = 0.4 nM) FK506. On the basis of the X-ray structure of FK506 bound to FKBP-12, it appears that such stabilizing interactions may be made by the side chains of His 87 and Ile 91 (Figure 5), which make hydrophobic contacts with the pyranose ring (C10–C14) of the bound ligand, as well as Tyr 82, which contacts the pyranose and hydrogen bonds to the C8 carbonyl (Van Duyne et al., 1991, 1993). These packing interactions are also illustrated in CPK representation in Figure 6. Contacts between loop residues and the drug molecule could also account for the changes in spectral intensities observed for residues 85 and 86 illustrated in Figure 3, as well as for Tyr 82 (not shown).

Structural Implications. As suggested previously (Cheng et al., 1993), it appears that interactions with the inhibitor are also responsible for stabilizing elements of secondary structure that are well-defined in the complex yet poorly defined in the native protein. This is particularly true in the "flap region" containing residues 78–95. For example, the solution structure reported for the FKBP-12/ascomycin complex contained a single turn of 3_{10} helix from residues 78 to 80 and two type II β-turns from residues 87 to 90 and 92 to 95 (Meadows et al., 1993). However, in uncomplexed FKBP-12, the flap region was not well-defined due to a lack of NOE restraints (Michnick et al., 1991; Moore et al., 1991). Evidence for conformational exchange in this region (Rosen et al., 1991) also presented problems for determination of solution structures for the uncomplexed protein. The decrease in mobility, or alternatively, the increase in rigidity of the 80's loop which occurs upon ligand binding, can explain why more restraints were obtained in this region for the ascomycin/FKBP-12 complex and, consequently, why the structure appeared better defined than those determined for the uncomplexed protein.

Solution Dynamics and Protein Function. Molecular motions occurring on many distinct time scales may be critical for protein function. Large-scale motions such as hinge bending in the glycolytic enzymes (Muirhead & Watson, 1993) or smaller scale domain or flap movements in, e.g., the aspartyl proteases and lipases (Davies, 1990; Smith et al., 1992) have been proposed to be necessary to allow access of ligands to otherwise closed active sites.

In a previous study (Cheng et al., 1993), we showed that a moderate degree of flexibility is inherent in uncomplexed FKBP-12. This flexibility is localized in the flap region of FKBP-12 and has been demonstrated experimentally by the low order parameters observed for residues in this loop. Upon inhibitor binding, the amplitudes of these motions are attenuated considerably and assume values close to the average order parameter for the complete protein. The observed flexibility of the flap region (80's loop) of FKBP-12 could facilitate access of substrates and ligands to the enzyme active site and hydrophobic binding core and could in part account for the relatively diverse substrate recognition of FKBP-12 (Park et al., 1992).

As described previously, mobility observed in the crystalline state, characterized by the crystallographic B factor (temperature factor), and mobility in solution, described by the generalized order parameter, do not always correlate (Cheng et al., 1993). Regions of the protein backbone in which true thermal motions are higher than average may be obscured or otherwise altered by the presence of crystal contacts. In the case of FKBP-12, one might easily be misled by the subtle changes observed between the crystal structures of the uncomplexed and complexed forms of FKBP-12, for which

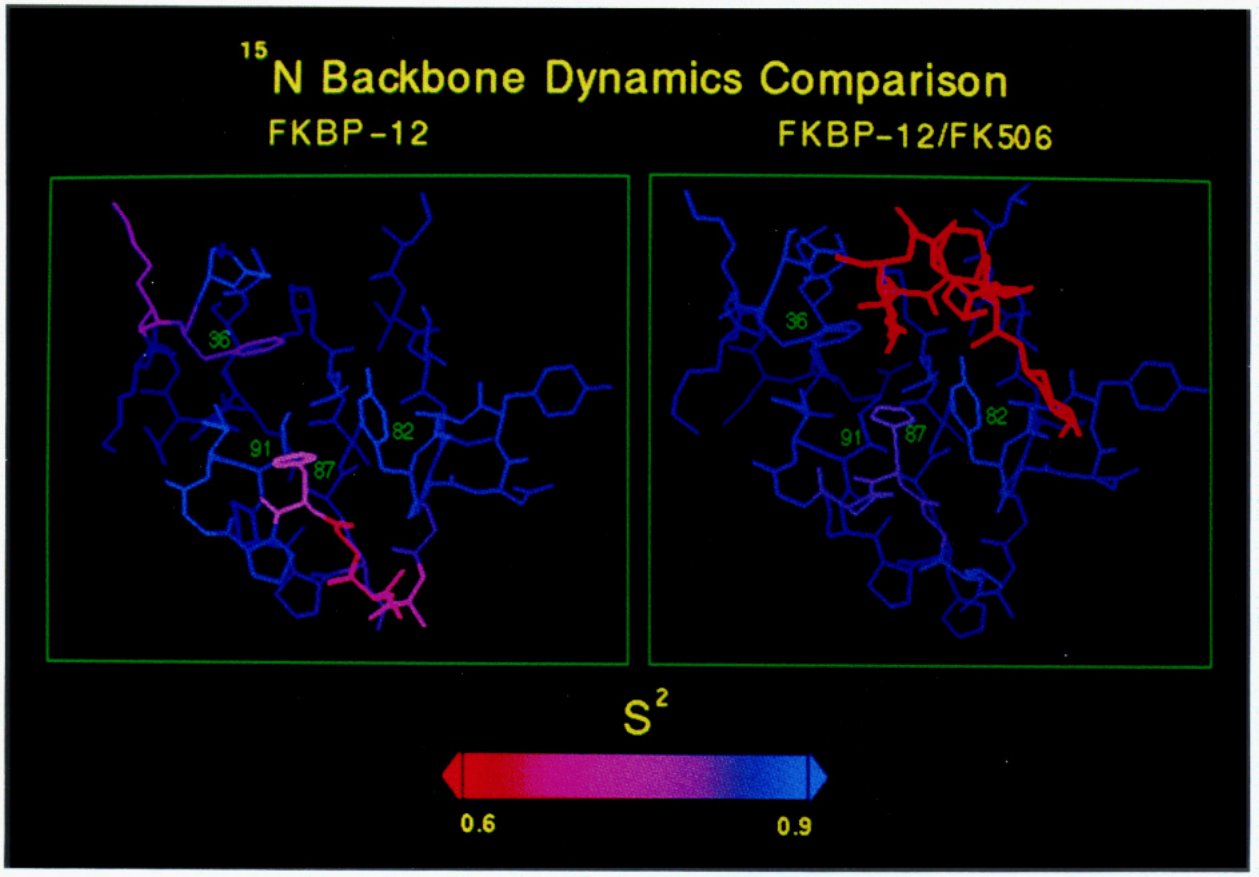

FIGURE 5: Close-up view of the flap region or 80's loop (bottom part of the structures shown in Figure 4) with side chains drawn. Several residues of FKBP-12 which make contact with FK506 are numbered. The spectrum bar below the structures indicates the color range and the values encompassed by each spectrum. Side chains are colored according to the order parameter observed at the amide position.

the RMS displacements between α-carbon atoms is only 0.48 Å (K. P. Wilson, M. M. Yamashita, S. H. Rotstein, M. A. Murcko, J. Boger, J. A. Thomson, M. J. Fitzgibbon, and M. A. Navia, unpublished results). Although these molecules appear to be almost identical structurally, dynamically they are quite distinct, and recognizing such differences in protein mobility may be critical to understanding protein function. In such instances, the parameters provided by ^{15}N relaxation studies to assess quantitatively molecular motions *in solution* add a "fourth dimension" to an otherwise three-dimensional (coordinate) representation of a protein target. Such studies may be invaluable in systems for which significant motions are proposed to be important mechanistically but cannot be directly demonstrated crystallographically.

Implications for Calcineurin Recognition. Inhibition of calcineurin by immunophilin/drug complexes has been demonstrated to be highly specific. Neither FKBP-12 nor cyclophilin alone, nor their free ligands (FK506 and CsA), appears to possess calcineurin inhibitory activity. Rather, only the Cyp/CsA and FKBP-12/FK506 complexes can bind to and inhibit calcineurin (Liu et al., 1991). Inhibition data for analogs of FK-506 (Liu et al., 1992) with modifications at the 15-methoxy and allyl groups suggest that these solvent-exposed regions (Lepre et al., 1992) are important for calcineurin recognition, and these data alone support the "effector domain" hypothesis of Schreiber as it was first proposed, namely, that regions of the FK506 molecule protruding from the protein surface in the FKBP-12/FK506 complex are responsible for the observed immunomodulatory effects (Schreiber, 1991). However, recent studies employing site-directed mutagenesis of selected FKBP-12 surface residues (Aldape et al., 1992; Yang et al., 1993) indicate that changes in the protein surface or protein/drug surface may also have profound effects on calcineurin inhibition. As a result of these studies, the effector domain hypothesis has evolved; it is now probable that regions of the ligand (FK506) and protein (FKBP-12) together form a calcineurin recognition surface.

How does the present work contribute to our understanding of the calcineurin inhibitory potential of the FKBP-12/FK506 complex? From the present studies, we conclude that backbone mobility in the 80's loop of FKBP-12 is attenuated upon ligand binding and that the entire protein backbone is rigidly fixed.[3] This structural rigidity extends to the bound ligand as well. In recent ^{13}C NMR dynamic studies of the receptor-bound FK506, we found that all methine sites on the main chain of the bound macrocycle possess high order parameters and, therefore, low mobility on the picosecond time scale (Lepre et al., 1993). Included in these sites were the solvent-exposed C21–C25 region, as well as the pyranose ring, which makes hydrophobic contacts with side chains of residues in the 80's loop. Together, these results imply that, with the exception of the allyl region, FKBP-12 and FK506 in the binary complex form a rigid, well-defined interface which is recognized by its downstream target, calcineurin. Although it is possible that such a rigid interface is *necessary* for immunosuppression, we may only conclude from our results that a relatively immobile interface is *sufficient* to achieve an immunosuppressive effect. One can propose, on the basis of the dynamic results in this and other studies (Lepre et al., 1993), that it is unlikely that the interaction with calcineurin

[3] Note that we are unable to characterize the mobility at proline residues or residues for which resonance overlap or low peak intensities preclude determination of the generalized order parameter.

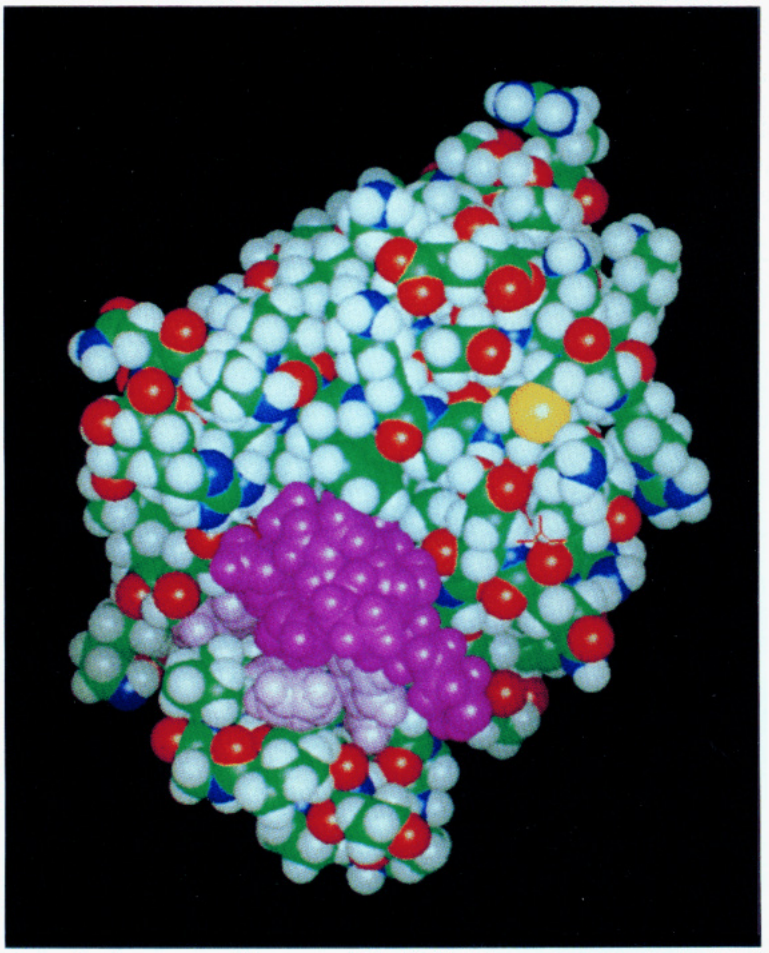

FIGURE 6: CPK representation of the FKBP-12/FK506 complex. The FK506 molecule is shown in magenta. Side chains of residues Phe 36, Tyr 82, His 87, and Ile 91 which are in close contact with the bound ligand are shown in violet below the drug molecule.

would significantly alter the structure of the FKBP-12/FK506 complex. In other words, it seems more plausible energetically that flexible regions of calcineurin would adapt to accommodate an already rigid binary FKBP-12/FK506 complex, rather than require the phosphatase to induce conformational changes in the structurally stable FKBP-12/FK506 protein–ligand interface. One possibility is that the highly mobile, hydrophobic allyl group binds in a hydrophobic cleft on the calcineurin complex, with the remainder of the macrocycle and the surrounding protein forming a complementary surface. This mode of binding would account for the decreased inhibitory activity observed for the "truncated allyl" FK506 analogs FK520 and FK523 (Liu et al., 1992) and the effects due to substitution at the 15-methoxy, as well as the differences in inhibitory potential due to site-directed mutagenesis of residues at the FKBP-12/FK506 interface. We eagerly await high-resolution structural data for the ternary FKBP-12/FK506/CN complex to determine if this is indeed the case.

Despite the absence of a high-resolution X-ray structure for the FKBP-12/FK506/CN complex, the ^{15}N dynamics results in this study provide valuable information for guiding the design of structure-based, FKBP-12-mediated calcineurin inhibitors. The structural rigidity observed for the FKBP-12/FK506 complex provides some assurance that use of the binary complex as an inhibitory model is justified. It follows that a successful route to the design of such inhibitors requires engineering a calcineurin recognition surface with structural rigidity in both the solvent-exposed regions of the bound ligand and the flap region (80's loop) of FKBP-12. Such strategies are currently being pursued in our own drug design efforts.

ACKNOWLEDGMENT

We thank Dr. Steve Chambers and John Fulghum for overexpression of FKBP-12 and Matthew Fitzgibbon and Dr. John Thomson for purification of FKBP-12 and preparation of the complex. We also thank Dr. Art Palmer, III, Dr. David Pearlman, and Jim Griffith for providing software routines and helpful discussions and Drs. Pat Connelly, David Livingston, Mark Murcko, and Manuel Navia for helpful discussions.

REFERENCES

Aldape, R. A., Futer, O., DeCenzo, M. T., Jarrett, B. P., Murcko, M. A., & Livingston, D. J. (1992) *J. Biol. Chem. 267*, 16029–16032.

Appelt, K., Bacquet, R. J., Bartlett, C. A., Booth, C. L. J., Freer, S. T., Fuhry, M. A. M., Gehring, M. R., Herrmann, S. M., Howland, E. F., Janson, C. A., Jones, T. R., Kan, C., Kathardekar, V., Lewis, K. K., Marzoni, G. P., Matthews, D. A., Mohr, C., Moomaw, E. W., Morse, C. A., Oatley, S. J., Ogden, R. C., Reddy, M. R., Reich, S. H., Schoettlin, W. S., Smith, W. W., Varney, M. D., Villafranca, J. E., Ward, R. W., Webber, S., Webber, S. E., Welsh, K. M., & White, J. (1991) *J. Med. Chem. 34*, 1925–1934.

Baldwin, J. J., Ponticello, G. S., Anderson, P. S., Christy, M. E., Murcko, M. A., Randall, W. C., Schwam, H., Sugrue, M. F., Springer, J. P., Gautheron, P., Grove, J., Mallorga, P., Viader, M., McKeever, B. M., & Navia, M. A. (1989) *J. Med. Chem. 32*, 2510–2513.

Bierer, B. E., Somers, P. K., Wandless, T. J., Burakoff, S. J., & Schreiber, S. L. (1990) *Science 250*, 556–559.

Cheng, J.-W., Lepre, C. A., Chambers, S., Fulghum, J. R., Thomson, J. A., & Moore, J. M. (1993) *Biochemistry 32*, 9000–9010.

Clore, G. M., Szabo, A., Bax, A., Kay, L. E., Driscoll, P. C., & Gronenborn, A. M. (1990) *J. Am. Chem. Soc. 112*, 4989–4991.

Davies, D. R. (1990) *Annu. Rev. Biophys. Biophys. Chem. 19*, 189–215.

Kay, L. E., Torchia, D. A., & Bax, A. (1989) *Biochemistry 28*, 8972–8979.

Kuntz, I. D. (1992) *Science 257*, 1078–1082.

Lepre, C. A., Thomson, J. A., & Moore, J. M. (1992) *FEBS Lett. 302*, 89–96.

Lepre, C. A., Cheng, J. -W., & Moore, J. M. (1993) *J. Am. Chem. Soc. 115*, 4929–4930.

Lipari, G., & Szabo, A. (1980) *Biophys. J. 30*, 489–506.

Lipari, G., & Szabo, A. (1981) *J. Chem. Phys. 75*, 2971–2976.

Lipari, G., & Szabo, A. (1982a) *J. Am. Chem. Soc. 104*, 4546–4559.

Lipari, G., & Szabo, A. (1982b) *J. Am. Chem. Soc. 104*, 4559–4570.

Liu, J., Farmer, J. D. J., Lane, W. S., Friedman, J., Weissman, I., & Schreiber, S. L. (1991) *Cell 66*, 807–815.

Liu, J., Albers, M. W., Wandless, T. J., Luan, S., Alberg, D. G., Belshaw, P. J., Cohen, P., Meadows, R. P., Nettesheim, D. G., Xu, R. X., Olejniczak, E. T., Petros, A. M., Holzman, T. F., Michnick, S. W., Rosen, M. K., Wandless, T. J., Karplus, M., & Schreiber, S. L. (1991) *Science 252*, 836.

Moore, J. M., Peattie, D. A., Fitzgibbon, M. J., & Thomson, J. A. (1991) *Nature 351*, 248–250.

Navia, M. A., & Murcko, M. A. (1992) *Curr. Opin. Struct. Biol. 2*, 202–210.

Palmer, A. G., III (1993) *Curr. Opin. Biotechnol. 4*, 385–391.

Palmer, A. G., III, Rance, M., & Wright, P. E. (1991) *J. Am. Chem. Soc. 113*, 4371–4380.

Park, S. T., Aldape, R. A., Futer, O., DeCenzo, M. T., & Livingston, D. L. (1992) *J. Biol. Chem. 267*, 3316–3324.

Rosen, M. K., & Schreiber, S. L. (1992) *Angew. Chem., Int. Ed. Engl. 31*, 384–400.

Rosen, M. K., Michnick, S. W., Karplus, M., & Schreiber, S. L. (1991) *Biochemistry 30*, 4774–4789.

Rosen, M. K., Yang, D., Martin, P. K., & Schreiber, S. L. (1993) *J. Am. Chem. Soc. 115*, 821–822.

Schreiber, S. L. (1991) *Science 251*, 283.

Sigal, N. H., & Dumont, F. J. (1992) *Annu. Rev. Immunol. 10*, 519–560.

Smith, L. C., Faustinella, F., & Chan, L. (1992) *Curr. Opin. Struct. Biol. 2*, 490–496.

Van Duyne, G. D., Standaert, R. F., Karplus, P. A., Schreiber, S. L., & Clardy, J. (1991) *Science 252*, 839.

Van Duyne, G. D., Standaert, R. F., Karplus, P. A., Schreiber, S. L., & Clardy, J. (1993) *J. Mol. Biol. 229*, 105–124.

Wagner, G. (1993) *Curr. Opin. Struct. Biol. 3*, 748–754.

Xu, R. X., Netteshem, D., Oleiniczak, E. T., Meadows, R., Gemmecker, G., & Fesik, S. W. (1993) *Biopolymers 33*, 535–550.

Yang, D., Rosen, M. K., & Schreiber, S. L. (1993) *J. Am. Chem. Soc. 115*, 819–820.